Transcriptomic analyses unveil the mechanism of saikosaponin A in inhibiting human neuroblastoma SK-N-AS cells

NING GAO[1,2], JIALIN SUN[3], WEI ZHAO[1,2], LIHUI DUAN[1,2], HONGYAO CAI[1,2], BO LIU[4*] and YUPENG CHENG[1,2*]

[1]Key Laboratory of Basic and Application Research of Beiyao, Heilongjiang University of Chinese Medicine, Ministry of Education, Harbin, Heilongjiang 150040, P.R. China; [2]School of Pharmacy, Heilongjiang University of Chinese Medicine, Harbin, Heilongjiang 150040, P.R. China; [3]Department of Medicine, Heilongjiang Minzu College, Harbin, Heilongjiang 150066, P.R. China; [4]School of Pharmaceutical Engineering, Heilongjiang Agricultural Reclamation Vocational College, Harbin, Heilongjiang 150025, P.R. China

Received September 11, 2024; Accepted May 8, 2025

DOI: 10.3892/ol.2025.15165

Abstract. Neuroblastoma (NB) is the most common pediatric malignant neoplasm. Saikosaponin A (SSa), a compound with potential therapeutic effects against this disease, inhibits the proliferation, metastasis and invasion of NB cells. However, its molecular mechanism remains elusive. The present study examined changes in gene expression in SK-N-AS NB cells after SSa administration using RNA sequencing. Subsequently, Gene Ontology (GO), Kyoto Encyclopedia of Genes and Genomes (KEGG) and Search Tool for the Retrieval of Interacting Genes/Proteins were used to analyze the differentially expressed genes between the treatment and control groups. Quantitative PCR technology confirmed the expression of the identified critical genes. The results identified multiple significant biological processes, including 717 GO terms and 55 KEGG pathways, constructing a 96-gene protein-protein interaction network, with *FN1* as the most relevant player in anti-NB mechanisms. The activities of SSa against NB were closely related to the regulations of the following genes: *IL24*, *EGR1*, *RET*, *MDK*, *PDGFRA*, *HGF*, *VCAM1*, *SLIT3*, *CD34*, *FN1*, *COL1A1* and *NCAM1*. Additionally, the PI3K-Akt signaling pathway was downregulated in the KEGG enriched results. Therefore, the results of the present study improves the critical understanding of the anti-NB mechanism of SSa and lays a foundation for its clinical application against NB.

Correspondence to: Mrs. Bo Liu, School of Pharmaceutical Engineering, Heilongjiang Agricultural Reclamation Vocational College, 660 Xueyuan Road, Limin Economic Development Zone, Harbin, Heilongjiang 150025, P.R. China
E-mail: 116123763@qq.com

Dr Yupeng Cheng, School of Pharmacy, Heilongjiang University of Chinese Medicine, 24 Heping Road, Xiangfang, Harbin, Heilongjiang 150040, P.R. China
E-mail: yupengcheng@msn.com

*Contributed equally

Key words: saikosaponin A, neuroblastoma, RNA-sequencing, antitumor activity

Introduction

Neuroblastoma (NB) is a type of cancer of the sympathetic nervous system characterized by extracranial solid tumors that arise from neural crest cells, and accounts for ~15% of cancer-related deaths in children (1,2). The median age at diagnosis is low (~18 months) with a notable number of cases occurring in infants (<1 year old for 40% of all NB cases) (3,4). Furthermore, over half of patients with NB are classified as high-risk, which results in a low 5-year survival rate (<50%) (3,4). The current major treatments for NB include spontaneous tumor regression, surgery, chemotherapy, radiotherapy and immunotherapy. Although therapy advancements have notably raised survival rates, the prognosis varies by the risk level (3,5-7). Furthermore, relapse, drug resistance and long-term side effects remain significant challenges for the treatment and recovery of these patients (8,9). Therefore, exploring new therapeutic drugs is of great clinical and scientific significance.

Multiple bioactivities have been reported for saikosaponin A (SSa), an oleanane-type saponin derived from *Bupleurum chinensis* DC. These include antitumor properties, anti-inflammatory effects and liver protection (10,11). Previous studies have shown that the antitumor activities of SSa, including suppressing cell proliferation, inducing apoptosis and inhibiting metastasis and angiogenesis, span various cell types including liver, colon, breast and pancreatic cancer cells (12). Specifically, in human hepatoma cell lines, SSa exhibits an antiproliferative effect (13,14). Such an effect in the HepG2 cell line is correlated with ERK activation and the upregulation of certain genes (15,16). In human colon carcinoma cells, SSa induces apoptosis by activating caspase-4, followed by activating sequential caspase-2 and -8 (17,18). In breast cancer cells, SSa inhibits proliferation and induces apoptosis (19,20). In both *in vitro* and *in vivo* conditions, SSa suppresses the activation of Akt and STAT3, decreases the levels of glycolysis and blocks the energy supply (21). In pancreatic cancer, SSa inhibits proliferation and induces

apoptosis, which may be related to the inactivation of the EGFR/PI3K/Akt pathway (22).

A study has shown that SSa inhibits the proliferation of NB cells by enhancing apoptosis (23). SSa decreases the expression of Bcl-2 and increases the expression of Bax while activating proteins such as caspase-9, caspase-7 and poly (ADP-ribose) polymerase (23). Furthermore, SSa stops NB cells from invading and migrating by blocking certain signals (such as VEGFR2, Src and Akt) and by regulating proteins connected with epithelial-mesenchymal transition (EMT) (23). However, the molecular mechanism of SSa against NB cell remains unclear. In the present study, human NB SK-N-AS cells were treated with SSa and the transcriptome expression profiles of these cells were analyzed using RNA-sequencing (seq) combined with bioinformatic methods. The differentially expressed genes (DEGs) were then verified by reverse transcription-quantitative PCR (RT-qPCR).

Materials and methods

Cell culture. The human SK-N-AS NB cell line was purchased from Heilongjiang Jiufeng Bioengineering Co., Ltd. The human SH-SY5Y NB cell line was purchased from Haixing Biosciences Co., Ltd. (Suzhou, China) and was authenticated by STR profiling. The human MO3.13 oligodendrocytic cell line (normal cells) was purchased from Cyagen Biosciences, Inc. These cells were initially cultured in Dulbecco's Modified Eagle Medium (DMEM; Gibco; Thermo Fisher Scientific, Inc.) containing 10% fetal bovine serum [FBS; Cellmax Cell Technology (Beijing) Co., Ltd.] and 1% penicillin-streptomycin (Gibco; Thermo Fisher Scientific, Inc.) in an incubator maintained at 37˚C with a humidified environment of 5% CO_2 and 95% air. Afterwards, cells were transferred every 2-3 days depending on their density, and experiments began once they achieved 80-90% confluency.

Cell viability assay. Cell viability was measured using the MTT assay following the protocol by Cheng and Ying (23). In brief, a cell suspension (SK-N-AS/SH-SY5Y/MO13.3) in DMEM containing 10% FBS (10^6 cells/ml) was inoculated into 96-well plates with 100 μl per well and cultured at 37˚C for 24 h with 5% CO_2 and 95% air. The cells were then treated with SSa (purity: HPLC ≥98%, Baoji Herbest Bio-Tech Co., Ltd.) at various concentrations [0 μM (control), 5, 10, 15, 20 and 25 μM] for 24 h. Following the treatment, 10 μl of MTT solution (5 mg/ml) was pipetted into each well, allowing the cells to incubate for an additional 4 h at 37˚C. The medium was discarded and 100 μl of DMSO was added to each well to dissolve the purple formazan while the absorbance was measured at 490 nm using a Microplate Reader (RT-6000; Rayto Life and Analytical Sciences Co., Ltd.). Cell viability was calculated as follows: Cell viability=[OD_{490} (SSa)/OD_{490} (control)] x100%.

Transwell migration and invasion assay. The methods were performed following the protocol by Cheng and Ying (23). In brief, SK-N-AS cells were digested and suspended in serum-free DMEM containing SSA (0 or 5 μM) at a final concentration of 10^6 cells/ml. For the invasion assay, 50 μl diluted Matrigel (Matrigel and serum-free DMEM were prepared at a ratio of 1:3 at 4˚C) was added to the upper Transwell chamber (24-well; pore size, 8 μm; Corning, Inc.) and incubated at 37˚C for 5 h. Subsequently, DMEM containing 20% FBS was added to the lower Transwell chamber. Subsequently, 100 μl of SK-N-AS cell suspension was plated in the upper chamber and incubated at 37˚C for 24 h. The cells that invaded into the lower surface of the Transwell membrane were fixed with 100% methanol (room temperature for 30 min) and stained with 0.1% crystal violet (room temperature for 20 min). Stained cells were observed by fluorescence inverted microscopy (Leica Microsystems GmbH). A total of five random fields were imaged to calculate the relative invasion rates based on the ratio of the number of invaded cells in the SSa group to the control group. For the migration assay, all the steps were the same as in the invasion assay but without the addition of Matrigel.

RNA isolation and sequencing. To isolate RNA, ~4 ml of SK-N-AS cells (10^6 cells/ml) were seeded into a T25 flask. The cells were cultured for ~2 days at standard conditions (37˚C for 48 h in humidified atmosphere of 5% CO_2 and 95% air) before being divided into two groups and treated for another 24 h: Those receiving SSa treatment (n=3) were incubated in FBS-free DMEM containing 15 μM SSa, and those in the control group did not receive any substance addition (n=3). Post-treatment, total RNA extraction from the SN-K-AS cells was performed using TRIzol Reagent (Invitrogen; Thermo Fisher Scientific, Inc.). NanoDrop spectrophotometer-based measurements (Thermo Fisher Scientific, Inc.) confirmed the concentration and purity levels alongside LabChip GX Touch HT Nucleic Acid analysis (PerkinElmer, Inc.).

The collected RNA samples (a total of 6, 3 for SSa treatment and 3 for control) were then transported to Wuhan Boyue Zhihe Biotechnology Co., Ltd., where library construction and sequencing tasks employing KAPA Stranded RNA-Seq Kit protocols plus multiplexing primer guidance were undertaken. In brief, mRNA was enriched by oligo(dT) beads and sequencing results were obtained using NovaSeq™ 6000 systems (Illumina, Inc.).

Data analysis. Raw data (raw reads) were filtered into clean data (clean reads) using Trimmomatic v0.36 (24). This involved removing reads with adapters, reads containing ploy-N and low-quality reads from the raw data. Clean data were then aligned to the human reference genome (http://asia.ensembl.org/Homo_sapiens/Info/Index) using Hisat 2 (25). The number of perfect clean tags for each gene was calculated and normalized as fragments per kilo bases per million mapped reads using featureCounts v1.5.0 (26). DEGs were identified using the DESeq R package (1.10.1) (27), with the following criteria: Fold-change ≥1.5 or ≤0.667 and adjusted $P<0.05$ (28).

Gene Ontology (GO) enrichment analysis was conducted by Database for Annotation, Visualization, & Integrated Discovery (DAVID) to reveal the biological function of DEGs (29,30). Kyoto Encyclopedia of Genes and Genomes (KEGG) was utilized to analyze the metabolic and signaling pathways inherent in the DEGs; enrichment and network construction were performed by Metascape 3.5 (31,32). Protein-protein interaction (PPI) networks of putative proteins encoded by DEGs were constructed with STRING 12.0 (33).

Table I. Primer sequences used in reverse transcription-quantitative PCR.

Gene	Forward primer (5'-3')	Reverse primer (5'-3')
IL24	TTGCCTGGGTTTTACCCTGC	AAGGCTTCCCACAGTTTCTGG
EGR1	GGTCAGTGGCCTAGTGAGC	GTGCCGCTGAGTAAATGGGA
RET	AAAGTGGCATTGGGCCTCTAC	GCAGGGCATGGACGTACAG
MDK	CGCGGTCGCCAAAAAGAAAG	TACTTGCAGTCGGCTCCAAAC
PDGFRA	TTGAAGGCAGGCACATTTACA	GCGACAAGGTATAATGGCAGAAT
HGF	GCTATCGGGGTAAAGACCTACA	CGTAGCGTACCTCTGGATTGC
VCAM1	CAGTAAGGCAGGCTGTAAAAGA	TGGAGCTGGTAGACCCTCG
SLIT3	GTCAGCGTCATCGAGAGAGG	TTCGGCGTGCTCTGGAAAAG
CD34	ACCAGAGCTATTCCCAAAAGACC	TGCGGCGATTCATCAGGAAAT
FN1	CGGTGGCTGTCAGTCAAAG	AAACCTCGGCTTCCTCCATAA
COL1A1	GTGCGATGACGTGATCTGTGA	CGGTGGTTTCTTGGTCGGT
NCAM1	GGCATTTACAAGTGTGTGGTTAC	TTGGCGCATTCTTGAACATGA
GAPDH	GGAGCGAGATCCCTCCAAAAT	GGCTGTTGTCATACTTCTCATGG

Validation by RT-qPCR. Total RNA was isolated from SK-N-AS cells using the SV Total RNA Isolation System (Promega Corporation), then reverse transcribed into cDNA using the GoScript™ kit (Promega Corporation) according to the manufacturer's protocol. qPCR was employed to assess DEG expression using the LineGene 9620 qPCR system (Hangzhou Bioer Co., Ltd.) following the GoTaq® qPCR protocol (Promega Corporation). The primer sequences for amplifying the DEGs are listed in Table I. Relative gene expression level was calculated based on the $2^{-\Delta\Delta Cq}$ method, with *GAPDH* as the internal control gene (34).

Statistical analysis. Data are presented as mean ± standard deviation. Student's unpaired t-test and one-way analysis of variance with Dunnett's post hoc test were applied for the statistical analyses of the cell viability and qPCR results. Fisher's exact test was used for bioinformatic analysis. $P<0.05$ was considered to indicate a statistically significant difference. Statistical analysis was performed using SPSS 26.0 (IBM Corp.).

Results

Inhibitory effect of SSa on human NB cells. As depicted in Fig. 1A and B, after 24 h, SSa reduced the viability of human SK-N-AS and SH-SY5Y NB cells in a dose-dependent manner. The half maximal inhibitory concentration values for SSa in SK-N-AS and SH-SY5Y cells after 24 h were 14.5 and 15.8 μM, respectively. SSa had no inhibitory effect on normal MO3.13 cells at doses <25 μM (Fig. 1C). This indicated that SSa was cytotoxic to SK-N-AS and SH-SY5Y cells and was non-toxic to normal cells at the effective doses, which aligned with the results of a previous study (23). In subsequent experiments, 15 μM was selected for transcriptomic analysis.

Inhibitory effect of SSa on the migration and invasion of SK-N-AS cells. Transwell assays were performed to verify the inhibitory effect of SSa on the migration and invasion of SK-N-AS cells. To prevent interference from the inhibitory effect of SSa on SK-N-AS cell viability, a concentration of SSa (5 μM) was used in these assays. As shown in Fig. 2, SSa significantly inhibited the migration and invasion of SK-N-AS cells, consistent with previous literature (23).

DEGs of SK-N-AS cells in the treatment and control groups. RNA-Seq was carried out to analyze the transcriptomic profile of the SK-A-AS cell samples, producing means of 42.5 million and 46.9 million clean reads for the control group and SSa treatment group, respectively. The overall mapped rates of clean reads to the human reference genome in all samples ranged from 92.41 to 94.68% (Table II). Compared with the control group, there were 297 DEGs in the SSa treatment group; among these genes, 23 were upregulated while 274 were downregulated (Table SI). The volcano plot in Fig. 3A illustrates the DEGs between the SSa treatment and control groups; genes were arranged based on their log2 fold change value along the x-axis and their-$\log_{10}$ adjusted P-value along the y-axis. A hierarchical clustered heatmap was created to visualize the gene expression relationship patterns between the samples. The 3 samples from each group were clustered on the same branch, indicating that SSa treatment significantly changed the gene expression patterns in SK-N-AS cells (Fig. 3B).

GO enrichment results of the DEGs. GO annotation enrichment analyses within the DEGs were assessed to determine the significant biological function changes. A total of 717 GO terms were enriched including 610 biological processes, 59 cellular components and 48 molecular functions. In the biological process category, 'cell adhesion' (GO: 0007155), 'biological adhesion' (GO: 0022610), 'neurogenesis' (GO: 0022008), 'extracellular matrix organization' (GO: 0030198) and 'extracellular structure organization' (GO: 0043062) were the top five significantly enriched processes. Biological processes related to the antitumor activity of SSa on human NB cells were also enriched, such as 'apoptotic process' (GO: 0006915), 'angiogenesis' (GO: 0001525) and 'epithelial to mesenchymal transition' (GO: 0001837). In the molecular function category, 'extracellular matrix structural component' (GO: 0005201), 'integrin binding'

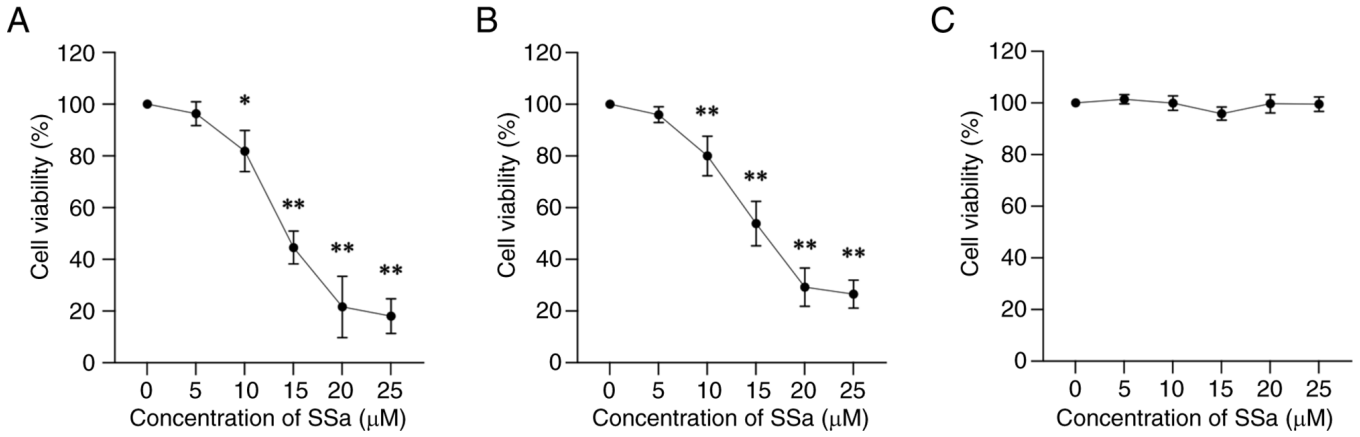

Figure 1. Viability of cells treated with various concentrations of SSa for 24 h. (A) Viability of the human SK-N-AS NB cell line treated with SSa. (B) Viability of the human SH-SY5Y NB cell line treated with SSa. (C) Viability of the human MO3.13 oligodendrocytic cell line (normal cells) treated with SSa. Data are displayed as the mean ± SD, n=6. *P<0.05, **P<0.01 vs. the 0 μM SSa group. NB, neuroblastoma; SSa, saikosaponin A.

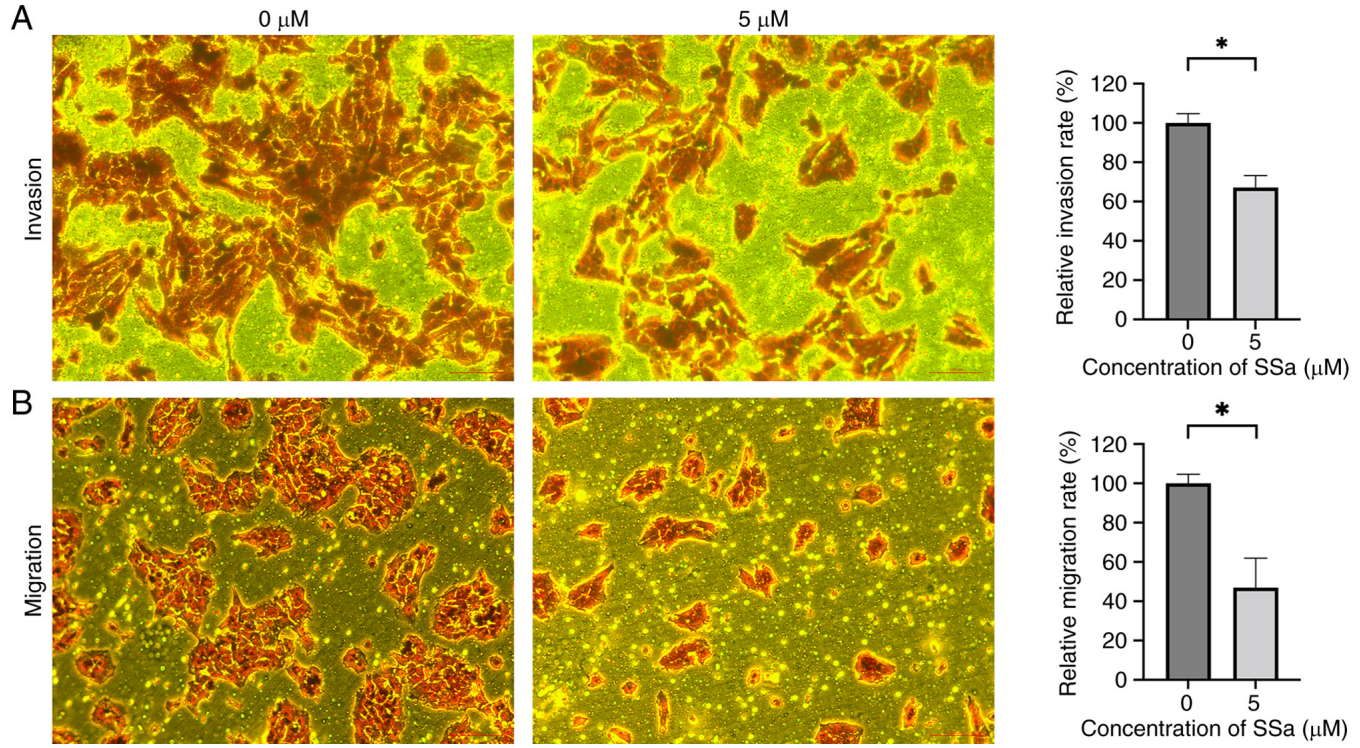

Figure 2. Invasion and migration of SK-N-AS cells treated with SSa for 24 h. (A) Transwell invasion assay images (magnification, x200) and the relative invasion rate of SK-N-AS cells treated with SSa (0 and 5 μM). (B) Transwell migration assay image (migration, x200) and the relative migration rate of SK-N-AS cells treated with SSa (0 and 5 μM). Data are displayed as mean ± SD, n=3. *P<0.05 vs. the 0 μM SSa group. SSa, saikosaponin A.

(GO: 0005178), 'glycosaminoglycan binding' (GO: 0005539), 'receptor binding' (GO: 0005102) and 'heparin binding' (GO: 0008201) represented the major functions encompassed by the DEGs. Moreover, in the cellular component category, the DEGs primarily contributed to 'extracellular matrix' (GO: 0031012), 'extracellular region' (GO: 0005576), 'extracellular region part' (GO: 0044421), 'cell surface' (GO: 0009986) and 'extracellular space' (GO: 0005615). Fig. 4 illustrates the top 20 GO terms within each category.

KEGG pathway enrichment results of the DEGs. The metabolic and signaling pathways contributing to SSa inhibition of SK-N-AS cells were also analyzed using the KEGG database. The results showed that the DEGs were enriched in 55 KEGG pathways (Table SII). Pathways related to the invasion and migration of cancerous cells were significantly enriched, such as 'ECM-receptor interaction' (hsa04512), 'Focal adhesion' (hsa04510) and 'Cell adhesion molecules' (hsa04514). In addition, 14 pathways belonged to signal transduction and 7 pathways were related to cancer. The signaling pathways included 'PI3K-Akt signaling pathway' (hsa04151), 'TNF signaling pathway' (hsa04668) and 'Apelin signaling pathway' (hsa04371). Cancer-related pathways included Metabolism of central carbon in cancer (hsa05230), 'Proteoglycans in cancer'

Table II. Alignment statistics of the reads aligned to the human reference genome.

Sample	Total clean reads	Total mapped reads	Uniquely mapped reads	Total mapped rate (%)
Control 1	41,986,280	39,101,793	36,821,952	93.13
Control 2	39,422,620	36,429,580	34,329,297	92.41
Control 3	46,085,672	42,722,112	40,263,786	92.70
SSa 1	42,659,786	39,484,619	37,215,349	92.56
SSa 2	39,815,270	37,695,401	35,546,191	94.68
SSa 3	58,333,588	54,581,167	51,362,190	93.57

SSa, saikosaponin A.

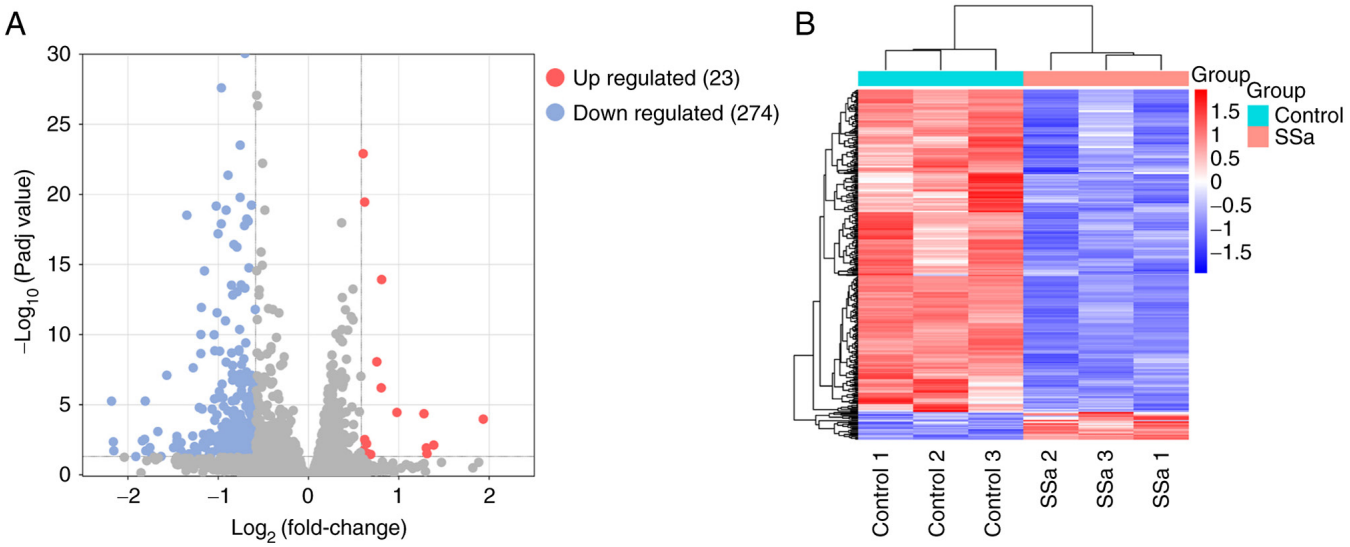

Figure 3. Analysis of the DEGs between the SSa treatment and control groups. (A) Volcano plot shows the expression level of each gene. The x-axis represents the $\log_2$ fold-change of the gene expression and the y-axis the represents-$\log_{10}$ P adj value. The red spots represent significantly upregulated DEGs and the blue spots represent significantly downregulated DEGs in the SSa treatment group compared with the control group. (B) Heatmap shows the gene expression pattern of each sample. The rows correspond to genes and the columns correspond to samples. DEGs, differentially expressed genes; SSa, saikosaponin A.

(hsa05205) and Non-small cell lung cancer (hsa05223). Other pathways mainly encompassed human disease and metabolic pathways. The top 20 significantly enriched pathways are shown in Fig. 5A, with connections among the enriched pathways shown as a network in Fig. 5B.

PPI networks based on the products of the DEGs. The list of gene symbols was submitted to the STRING database to construct the PPI network of putative proteins encoded by the DEGs, with 'organisms' set to *Homo sapiens* and the 'minimum required interaction score' set to high confidence. As shown in Fig. 6, the largest network contained 98 nodes and 201 edges, while 139 isolated nodes without any connections were hidden. Genes such as *FN1, COL1A1, DDX58, PTPRC, THBS1, CCL2, IFIH1, IL1B, MX1* and *VCAM1* ranked among the 10 most-connected genes and acted as hubs in the network. A total of 29 clusters were obtained based on Markov clustering, with the largest cluster containing 21 genes whose functions mainly referred to cell adhesion (hsa04512, hsa04514, hsa04510, GO:0007155, GO:0030155 and GO:0016477).

Confirmation of transcriptomic sequencing with qPCR. To verify the transcriptomic sequencing results, genes related to the SSa inhibition of SK-N-AS cells were determined by qPCR. These genes included *IL24*, *EGR1*, *RET*, *MDK*, *PDGFRA*, *HGF*, *VCAM1*, *SLIT3*, *CD34*, *FN1*, *COL1A1* and *NCAM1*. In the group treated with SSa, certain gene expression levels increased (*IL24* and *EGR1*) or decreased (*RET*, *MDK*, *PDGFRA*, *HGF*, *VCAM1*, *SLIT3*, *CD34*, *FN1*, *COL1A1* and *NCAM1*) significantly compared with the control group (Fig. 7). Therefore, the RNA-seq and qPCR data were consistent.

Discussion

SSa is one of the main active components of *Bupleurum chinensis* DC (10,11). In the present study, the antitumor activity of SSa on human NB cells (SK-N-AS and SH-SY5Y) and the absence of SSa inhibition on normal cells (MO3.13) was verified at the effective concentrations, indicating its safety. The inhibitory effects of SSa on SK-N-AS migration and invasion were also confirmed by Transwell assay. Furthermore, RNA-seq was performed in conjunction

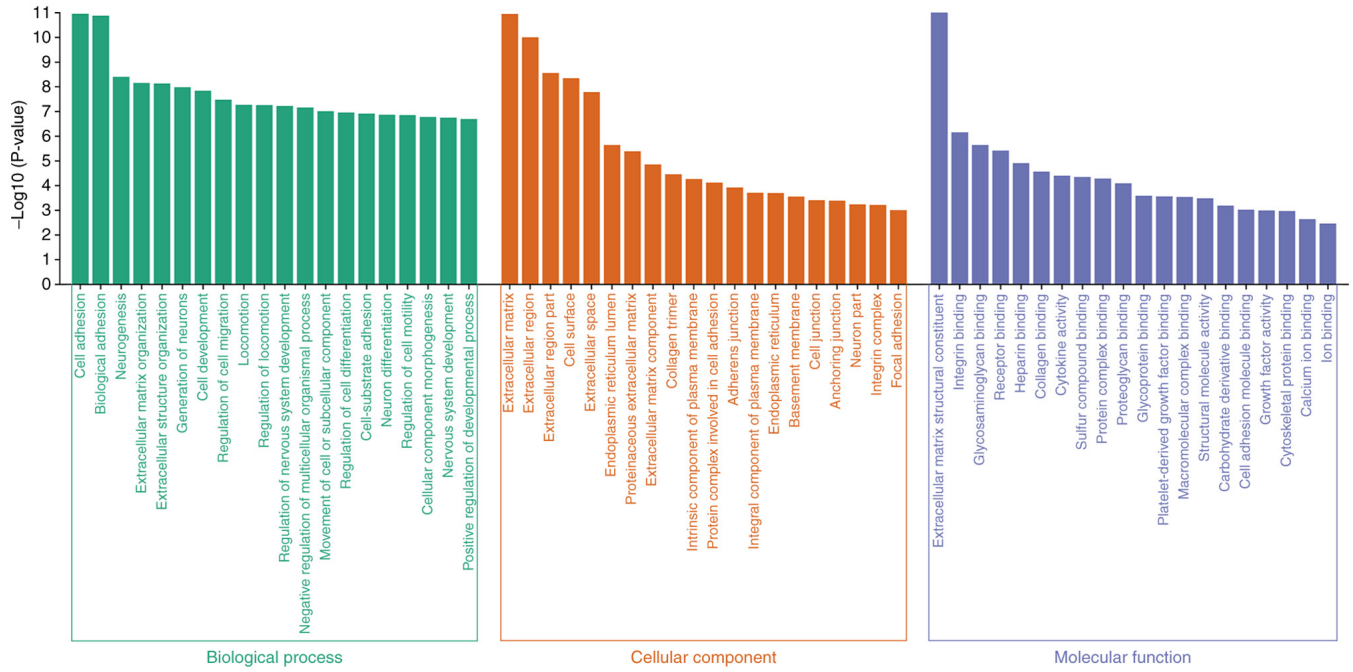

Figure 4. Enrichment results of the Gene Ontology terms associated with differentially expressed genes between the saikosaponin A treatment and control group.

with bioinformatics analysis, which revealed the molecular mechanism underlying the antitumor effects of SSa against NB at the mRNA level. As shown in the GO enrichment results, DEGs involved in apoptosis were enriched under the GO term GO:0006915 (apoptosis). The RNA-seq results alongside the qPCR verification indicated that the upregulated genes were *IL24* and *EGR1* and the downregulated genes were *RET* and *MDK*, which was consistent with the apoptosis pathway detected following GO enrichment, as indicated in previous studies (35-39). These results suggested that SSa may be an inhibitor of *RET* and *MDK* expression, and hence against NB. Notably, *RET* has been shown to be expressed in numerous NB cells (40), and its activation inhibits apoptosis in NB cells (38). RET inhibition is a promising antitumor therapeutic strategy and drugs targeting RET have shown promising effects in NB (41,42). As to *MDK*, some therapeutic strategies aimed at inhibiting *MDK* expression have also shown promising antitumor effects (43-45). In NB, increased MDK levels are correlated with an unfavorable prognosis, and reducing MDK expression may serve as an effective strategy for NB treatment (39).

In the present study, DEGs linked to angiogenesis were enriched under the GO term GO:0001525 (angiogenesis). The RNA-seq results alongside the qPCR verification indicated that the downregulated genes were *PDGFRA*, *HGF*, *VCAM1*, *SLIT3* and *CD34* after SSa treatment, which was consistent with the angiogenesis pathway detected in the GO enrichment, as suggested in previous studies (46-50). SSa could inhibit angiogenesis in NB by targeting the *PDGFRA* and *HGF* genes (and thus HGF/c-MET signaling). Notably, upregulation of *PDGFRA* has been observed in a number of malignancies and is associated with poor prognosis (51,52). Additionally, *HGF* promotes angiogenesis in NB and reports suggest that inhibiting the HGF/c-MET signaling pathway may have therapeutic effects against neuroblastoma (47,53). Meanwhile, *VCAM1* and *SLIT3* may be proangiogenic factors (48,54), and *CD34* has been used as a marker in immunohistochemistry to assess angiogenesis in tumors (50,55). However, the roles of *VCAM1*, *SLIT3* and *CD34* in the tumorigenesis of NB are currently unknown. In addition, the PI3K-Akt signaling pathway was downregulated according to the KEGG enrichment results obtained in the present study. This pathway influences angiogenesis by activating multiple angiogenic factors and its activation involves both *PDGFRA* and *HGF* (56,57). These findings suggest that SSa may suppress angiogenesis by inhibiting the PI3K-Akt signaling pathway, consistent with previous reports (22,23). The results of the present study also showed that after SSa treatment, the ECM-receptor interaction (hsa04512) in NB cells was the most significantly enriched KEGG pathway, which is closely linked to angiogenesis (GO:0001525). This ECM-receptor interaction pathway participates in the regulation of EMT progression, which is critical for metastasis (58). The expression levels of the *FN1*, *COL1A1* and *NCAM1* genes are all related to the EMT process (59-61).

In the present study, the PPI network results showed that the proteins in the extracellular matrix (FN1 and COL1A1) were the most connected proteins. Meanwhile, the RNA-seq results alongside the qPCR verification showed that the corresponding *FN1* and *COL1A1* genes were both downregulated in the treatment group. These results suggest that SSa could inhibit the metastasis-related EMT process by targeting *FN1* and *COL1A1*. The PPI network analysis also demonstrated that the largest protein cluster primarily encompassed cell adhesion. Consistently, the RNA-seq results alongside the qPCR verification showed that after SSa treatment, the cell adhesion molecule gene, *NCAM1*, was downregulated in NB cells. Therefore, SSa could inhibit the metastasis-related EMT process by suppressing the expression of *NCAM1*. Notably,

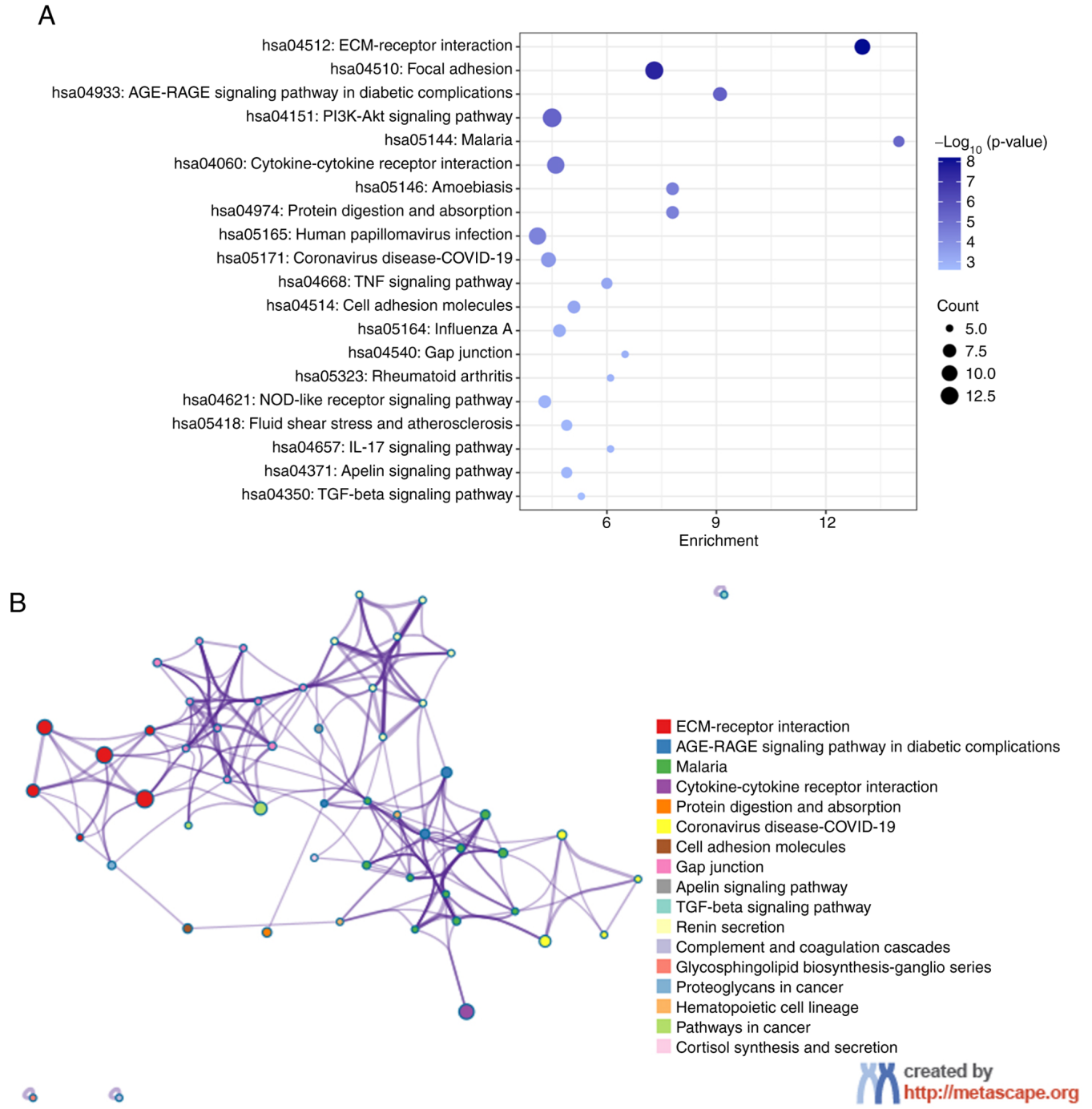

Figure 5. Enrichment results of the Kyoto Encyclopedia of Genes and Genomes pathway analysis involving differentially expressed genes between the saikosaponin A treatment and control groups. (A) Bubble diagram of the top 20 significantly enriched pathways. (B) Network diagram illustrating the connections among the enriched pathways.

the FN1 and COL1A1 proteins (and the corresponding genes) could be potential targets for cancer treatment (62-64), with NCAM1 more specifically for NB (65,66).

There are certain limitations of the present study. The present study only focused on the impact of SSa on SK-N-AS cells. Given the varying genetic makeup of different NB cells (2), further research is needed to determine whether the findings can be generalized to other NB cells. The present study elucidated the mechanism of SSa against NB at the transcriptional level. However, examination at the protein level is equally crucial for the determining the antitumor activity of the drug. Taking the aforementioned PI3K-Akt signaling pathway as an example, in addition to expression levels, the phosphorylation status of core proteins also plays a vital role in pathway activation. Therefore, further investigation is warranted to gain deeper insights into the molecular mechanisms underlying the anti-neuroblastoma effects of SSa. Additionally, subsequent animal studies should be performed to facilitate the clinical translation of SSA for neuroblastoma treatment.

In conclusion, the results of the present study showed that SSa significantly inhibited the viability, migration and

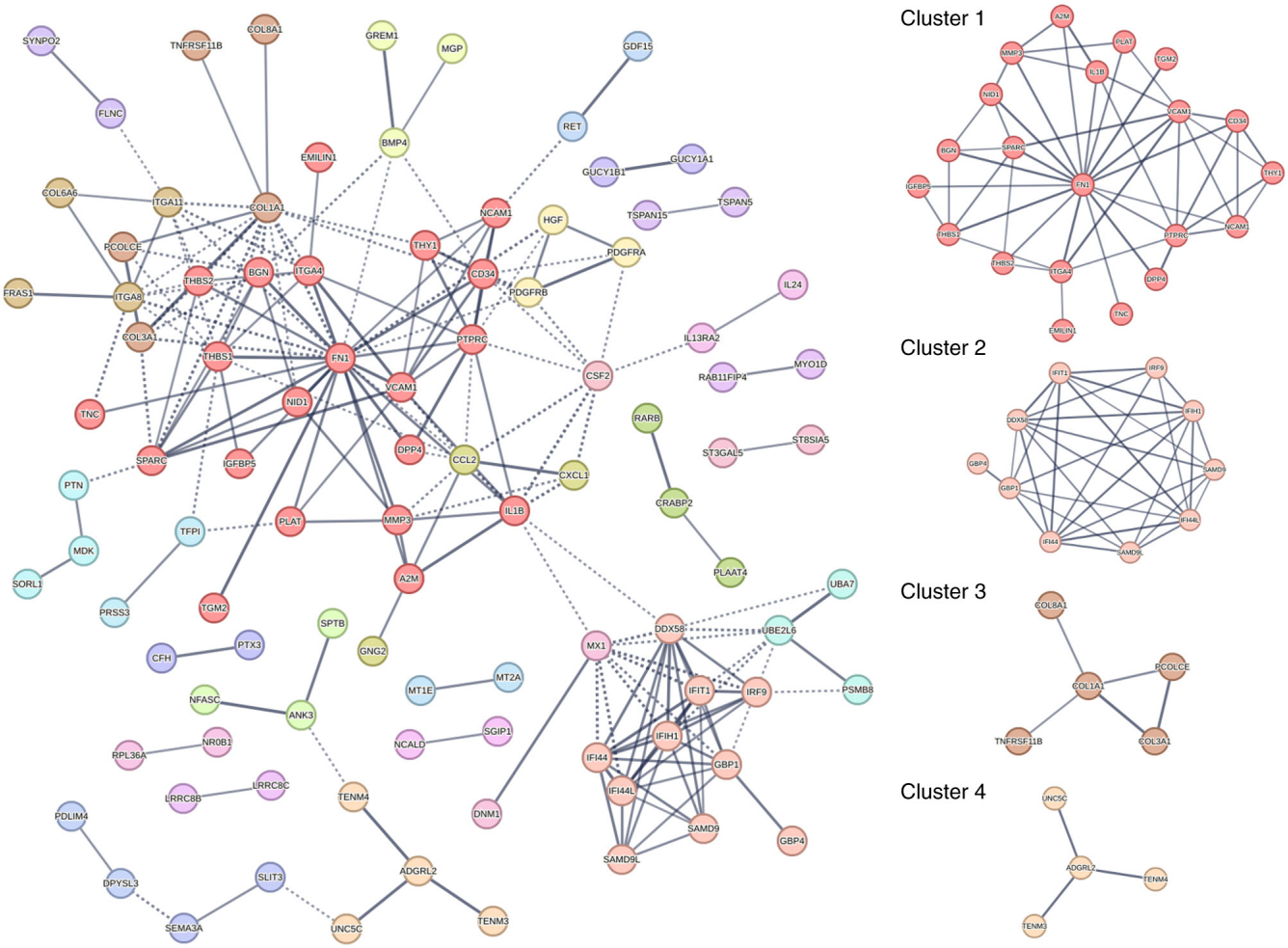

Figure 6. Protein-protein interaction network of differentially expressed genes between the saikosaponin A treatment and control groups, with the four largest clusters based on the Markov clustering shown on the right.

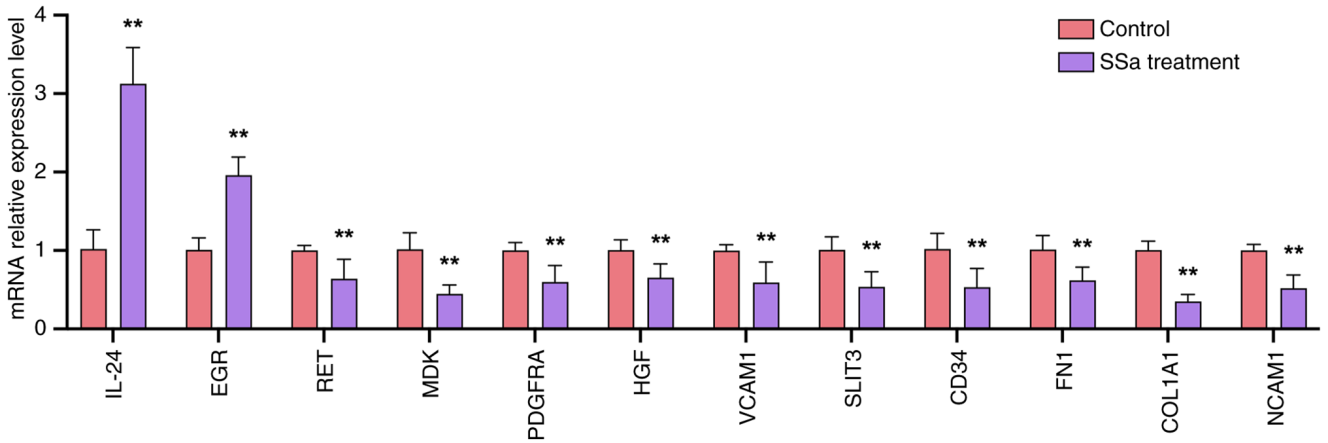

Figure 7. Relative expression levels of candidate genes validated by reverse transcription-quantitative PCR. Data is shown as mean ± SD, n=6 for all groups. **P<0.01 vs. control group. SSa, saikosaponin A.

invasion of SK-N-AS NB cells within 24 h. SSa likely induced apoptosis in SK-N-AS cells by upregulating *IL24* and *EGR1* and downregulating *RET* and *MDK* expression. SSa may have anti-angiogenesis effects through downregulating *PDGFRA*, *HGF*, *VCAM1*, *SLIT3* and *CD34*. SSa may suppress metastasis by inhibiting EMT through downregulating *FN1* (central hub), *COL1A1* and *NCAM1* expression as well as downregulating the PI3K-Akt signaling pathway. Therefore, the present study provided an in-depth comprehension of the molecular processes and signal transduction pathways driving the effects of SSa against NB through RNA-seq and bioinformatics analyses. However, the specific role of the relevant genes in the

anti-NB process of SSa and the direct target of SSa still needs further investigation. These findings suggest that SSa can be a potential therapeutic agent for NB.

Acknowledgements

Not applicable.

Funding

This work was supported by the National Natural Science Foundation of China (grant nos. 81503271 and 81573539), University Nursing Program for Young Scholars with Creative Talents in Heilongjiang Province (grant no. UNPYSCT-2017217) and the Heilongjiang Touyan Innovation Team Program [grant no. (2019) No. 5].

Availability of data and materials

The RNA-seq data generated in the present study may be found in the Sequence Read Archive database under accession no. PRJNA1158969 or at the following URL: https://www.ncbi.nlm.nih.gov/bioproject/PRJNA1158969. All other data generated in the present study may be requested from the corresponding author.

Authors' contributions

NG was responsible for study design and contributed to data interpretation. WZ, LD and HC performed the experiments. JS, BL and YC analyzed the data and modified the manuscript. BL and YC confirm the authenticity of all the raw data. All authors read and approved the final version of the manuscript.

Ethics approval and consent to participate

Not applicable.

Patient consent for publication

Not applicable.

Competing interest

The authors declare that they have no competing interests.

References

1. Zafar A, Wang W, Liu G, Xian W, McKeon F, Zhou J and Zhang R: Targeting the p53-MDM2 pathway for neuroblastoma therapy: Rays of hope. Cancer Lett 496: 16-29, 2021.
2. Bansal M, Gupta A and Ding HF: MYCN and metabolic reprogramming in neuroblastoma. Cancers (Basel) 14: 4113, 2022.
3. Zafar A, Wang W, Liu G, Wang X, Xian W, McKeon F, Foster J, Zhou J and Zhang R: Molecular targeting therapies for neuroblastoma: Progress and challenges. Med Res Rev 41: 961-1021, 2021.
4. Lundberg KI, Treis D and Johnsen JI: Neuroblastoma heterogeneity, plasticity, and emerging therapies. Curr Oncol Rep 24: 1053-1062, 2022.
5. Lin L, Miao L, Lin H, Cheng J, Li M, Zhuo Z and He J: Targeting RAS in neuroblastoma: Is it possible? Pharmacol Ther 236: 108054, 2022.
6. Qiu B and Matthay KK: Advancing therapy for neuroblastoma. Nat Rev Clin Oncol 19: 515-533, 2022.
7. Whittle SB, Smith V, Doherty E, Zhao S, McCarty S and Zage PE: Overview and recent advances in the treatment of neuroblastoma. Expert Rev Anticancer Ther 17: 369-386, 2017.
8. Rivera Z, Escutia C, Madonna MB and Gupta KH: Biological insight and recent advancement in the treatment of neuroblastoma. Int J Mol Sci 24: 8470, 2023.
9. Gao J, Fosbrook C, Gibson J, Underwood TJ, Gray JC and Walters ZS: Review: Targeting EZH2 in neuroblastoma. Cancer Treat Rev 119: 102600, 2023.
10. Li X, Li X, Huang N, Liu R and Sun R: A comprehensive review and perspectives on pharmacology and toxicology of saikosaponins. Phytomedicine 50: 73-87, 2018.
11. Li XQ, Song YN, Wang SJ, Rahman K, Zhu JY and Zhang H: Saikosaponins: A review of pharmacological effects. J Asian Nat Prod Res 20: 399-411, 2018.
12. Xiao LX, Zhou HN and Jiao ZY: Present and future prospects of the anti-cancer activities of saikosaponins. Curr Cancer Drug Targets 23: 2-14, 2022.
13. Motoo Y and Sawabu N: Antitumor effects of saikosaponins, baicalin and baicalein on human hepatoma cell lines. Cancer Lett 86: 91-95, 1994.
14. Qian L, Murakami T, Kimura Y, Takahashi M and Okita K: Saikosaponin A-induced cell death of a human hepatoma cell line (HuH-7): The significance of the 'sub-G1 peak' in a DNA histo. Pathol Int 45: 207-214, 1995.
15. Wen-Sheng W: ERK signaling pathway is involved in p15INK4b/p16INK4a expression and HepG2 growth inhibition triggered by TPA and saikosaponin A. Oncogene 22: 955-963, 2003.
16. Wu WS and Hsu HY: Involvement of p-15(INK4b) and p-16(INK4a) gene expression in saikosaponin a and TPA-induced growth inhibition of HepG2 cells. Biochem Biophys Res Commun 285: 183-187, 2001.
17. Kang SJ, Lee YJ, Kang SG, Cho S, Yoon W, Lim JH, Min SH, Lee TH and Kim BM: Caspase-4 is essential for saikosaponin a-induced apoptosis acting upstream of caspase-2 and γ-H2AX in colon cancer cells. Oncotarget 8: 100433-100448, 2017.
18. Kim BM and Hong SH: Sequential caspase-2 and caspase-8 activation is essential for saikosaponin a-induced apoptosis of human colon carcinoma cell lines. Apoptosis 16: 184-197, 2011.
19. Chen JC, Chang NW, Chung JG and Chen KC: Saikosaponin-A induces apoptotic mechanism in human breast MDA-MB-231 and MCF-7 cancer cells. Am J Chin Med 31: 363-377, 2003.
20. Zhao X, Liu J, Ge S, Chen C, Li S, Wu X, Feng X, Wang Y and Cai D: Saikosaponin A inhibits breast cancer by regulating Th1/Th2 balance. Front Pharmacol 10: 624, 2019.
21. Zhang Y, Dai K, Xu D, Fan H, Ji N, Wang D, Zhao Y and Liu R: Saikosaponin A alleviates glycolysis of breast cancer cells through repression of Akt/STAT3 pathway. Chem Biol Drug Des 102: 115-125, 2023.
22. Shi C, Sun L, Fang R, Zheng S, Yu M and Li Q: Saikosaponin-A exhibits antipancreatic cancer activity by targeting the EGFR/PI3K/Akt pathway. Curr Pharm Biotechnol 24: 579-588, 2023.
23. Cheng T and Ying M: Antitumor effect of Saikosaponin A on human neuroblastoma cells. Biomed Res Int 2021: 5845554, 2021.
24. Bolger AM, Lohse M and Usadel B: Trimmomatic: A flexible trimmer for illumina sequence data. Bioinformatics 30: 2114-2120, 2014.
25. Kim D, Paggi JM, Park C, Bennett C and Salzberg SL: Graph-based genome alignment and genotyping with HISAT2 and HISAT-genotype. Nat Biotechnol 37: 907-915, 2019.
26. Liao Y, Smyth GK and Shi W: featureCounts: An efficient general purpose program for assigning sequence reads to genomic features. Bioinformatics 30: 923-930, 2014.
27. Anders S and Huber W: Differential expression analysis for sequence count data. Genome Biol 11: R106, 2010.
28. Robinson MD, McCarthy DJ and Smyth GK: EdgeR: A Bioconductor package for differential expression analysis of digital gene expression data. Bioinformatics 26: 139-140, 2010.
29. Gene Ontology Consortium; Aleksander SA, Balhoff J, Carbon S, Cherry JM, Drabkin HJ, Ebert D, Feuermann M, Gaudet P, Harris NL, *et al*: The gene ontology knowledgebase in 2023. Genetics 224: iyad031, 2023.
30. Sherman BT, Hao M, Qiu J, Jiao X, Baseler MW, Lane HC, Imamichi T and Chang W: DAVID: A web server for functional enrichment analysis and functional annotation of gene lists (2021 update). Nucleic Acids Res 50: W216-W221, 2022.

31. Kanehisa M, Furumichi M, Sato Y, Kawashima M and Ishiguro-Watanabe M: KEGG for taxonomy-based analysis of pathways and genomes. Nucleic Acids Res 51: D587-D592, 2023.
32. Zhou Y, Zhou B, Pache L, Chang M, Khodabakhshi AH, Tanaseichuk O, Benner C and Chanda SK: Metascape provides a biologist-oriented resource for the analysis of systems-level datasets. Nat Commun 10: 1523, 2019.
33. Szklarczyk D, Gable AL, Lyon D, Junge A, Wyder S, Huerta-Cepas J, Simonovic M, Doncheva NT, Morris JH, Bork P, *et al*: STRING v11: Protein-protein association networks with increased coverage, supporting functional discovery in genome-wide experimental datasets. Nucleic Acids Res 47: D607-D613, 2019.
34. Livak KJ and Schmittgen TD: Analysis of relative gene expression data using real-time quantitative PCR and the 2(-Delta Delta C(T)) method. Methods 25: 402-408, 2001.
35. Pignatelli M, Luna-Medina R, Pérez-Rendón A, Santos A and Perez-Castillo A: The transcription factor early growth response factor-1 (EGR-1) promotes apoptosis of neuroblastoma cells. Biochem J 373: 739-746, 2003.
36. Cibelli G, Policastro V, Rössler OG and Thiel G: Nitric oxide-induced programmed cell death in human neuroblastoma cells is accompanied by the synthesis of Egr-1, a zinc finger transcription factor. J Neurosci Res 67: 450-460, 2002.
37. Li Y, Zhang H, Zhu X, Feng D, Gong J and Han T: Interleukin-24 induces neuroblastoma SH-SY5Y cell differentiation, growth inhibition, and apoptosis by promoting ROS production. J Interferon Cytokine Res 33: 709-714, 2013.
38. Skinner MA, Lackey KE and Freemerman AJ: RET activation inhibits doxorubicin-induced apoptosis in SK-N-MC cells. Anticancer Res 28: 2019-2025, 2008.
39. Kishida S and Kadomatsu K: Involvement of midkine in neuroblastoma tumourigenesis. Br J Pharmacol 171: 896-904, 2014.
40. Futami H and Sakai R: RET protein promotes non-adherent growth of NB-39-nu neuroblastoma cell line. Cancer Sci 100: 1034-1039, 2009.
41. Steen EA, Basilaia M, Kim W, Getz T, Gustafson JL and Zage PE: Targeting the RET tyrosine kinase in neuroblastoma: A review and application of a novel selective drug design strategy. Biochem Pharmacol 216: 115751, 2023.
42. Ishida M, Ichihara M, Mii S, Jijiwa M, Asai N, Enomoto A, Kato T, Majima A, Ping J, Murakumo Y and Takahashi M: Sprouty2 regulates growth and differentiation of human neuroblastoma cells through RET tyrosine kinase. Cancer Sci 98: 815-821, 2007.
43. Erdogan S, Doganlar ZB, Doganlar O, Turkekul K and Serttas R: Inhibition of midkine suppresses prostate cancer $CD133^+$ stem cell growth and migration. Am J Med Sci 354: 299-309, 2017.
44. Hao H, Maeda Y, Fukazawa T, Yamatsuji T, Takaoka M, Bao XH, Matsuoka J, Okui T, Shimo T, Takigawa N, *et al*: Inhibition of the growth factor MDK/midkine by a novel small molecule compound to treat non-small cell lung cancer. PLoS One 8: e71093, 2013.
45. Han X, Li M, Xu J, Fu J, Wang X, Wang J, Xia T, Wang S and Ma G: miR-1275 targets MDK/AKT signaling to inhibit breast cancer chemoresistance by lessening the properties of cancer stem cells. Int J Biol Sci 19: 89-103, 2023.
46. Hou Y, Du W, Wu Q, Chai X, Wang Y, Mi Y, Tian Y, Tang M, Li J and Yan D: PDGFRA exhibits potential as an indicator of angiogenesis within the tumor microenvironment and is up-regulated in BLCA. Microvasc Res 151: 104614, 2024.
47. Daudigeos-Dubus E, LeDret L, Bawa O, Opolon P, Vievard A, Villa I, Bosq J, Vassal G and Geoerger B: Dual inhibition using cabozantinib overcomes HGF/MET signaling mediated resistance to pan-VEGFR inhibition in orthotopic and metastatic neuroblastoma tumors. Int J Oncol 50: 203-211, 2017.
48. Xiang X, Pathak JL, Wu W, Li J, Huang W, Wu Q, Xin M, Wu Y, Huang Y, Ge L and Zeng S: Human serum-derived exosomes modulate macrophage inflammation to promote VCAM1-mediated angiogenesis and bone regeneration. J Cell Mol Med 27: 1131-1143, 2023.
49. Yallowitz AR, Shim JH, Xu R and Greenblatt MB: An angiogenic approach to osteoanabolic therapy targeting the SHN3-SLIT3 pathway. Bone 172: 116761, 2023.
50. Sasano H and Suzuki T: Pathological evaluation of angiogenesis in human tumor. Biomed Pharmacother 59 (Suppl 2): S334-S336, 2005.
51. Lin LH, Lin JS, Yang CC, Cheng HW, Chang KW and Liu CJ: Overexpression of platelet-derived growth factor and its receptor are correlated with oral tumorigenesis and poor prognosis in oral squamous cell carcinoma. Int J Mol Sci 21: 2360, 2020.
52. Wei T, Zhang LN, Lv Y, Ma XY, Zhi L, Liu C, Ma F and Zhang XF: Overexpression of platelet-derived growth factor receptor alpha promotes tumor progression and indicates poor prognosis in hepatocellular carcinoma. Oncotarget 5: 10307-10317, 2014.
53. Hecht M, Papoutsi M, Tran HD, Wilting J and Schweigerer L: Hepatocyte growth factor/c-Met signaling promotes the progression of experimental human neuroblastomas. Cancer Res 64: 6109-6118, 2004.
54. Paul JD, Coulombe KLK, Toth PT, Zhang Y, Marsboom G, Bindokas VP, Smith DW, Murry CE and Rehman J: SLIT3-ROBO4 activation promotes vascular network formation in human engineered tissue and angiogenesis in vivo. J Mol Cell Cardiol 64: 124-131, 2013.
55. Liu H and Zhao KY: Application of CD34 expression combined with three-phase dynamic contrast-enhanced computed tomography scanning in preoperative staging of gastric cancer. World J Gastrointest Surg 15: 2513-2524, 2023.
56. Mei Y, Wang Z, Zhang L, Zhang Y, Li X, Liu H, Ye J and You H: Regulation of neuroblastoma differentiation by forkhead transcription factors FOXO1/3/4 through the receptor tyrosine kinase PDGFRA. Proc Natl Acad Sci USA 109: 4898-4903, 2012.
57. Moosavi F, Giovannetti E, Peters GJ and Firuzi O: Combination of HGF/MET-targeting agents and other therapeutic strategies in cancer. Crit Rev Oncol Hematol 160: 103234, 2021.
58. An Q, Liu T, Wang MY, Yang YJ, Zhang ZD, Lin ZJ and Yang B: CircKRT7-miR-29a-3p-COL1A1 axis promotes ovarian cancer cell progression. Onco Targets Ther 13: 8963-8976, 2020.
59. Dehghan MH, Ashrafi MR, Hedayati M, Shivaee S and Rajabi S: Oral contraceptive steroids promote papillary thyroid cancer metastasis by targeting angiogenesis and epithelial-mesenchymal transition. Int J Mol Cell Med 10: 219-226, 2021.
60. Li X, Sun X, Kan C, Chen B, Qu N, Hou N, Liu Y and Han F: COL1A1: A novel oncogenic gene and therapeutic target in malignancies. Pathol Res Pract 236: 154013, 2022.
61. Li J, Yang R, Yang H, Chen S, Wang L, Li M, Yang S, Feng Z and Bi J: NCAM regulates the proliferation, apoptosis, autophagy, EMT, and migration of human melanoma cells via the Src/Akt/mTOR/cofilin signaling pathway. J Cell Biochem 121: 1192-1204, 2020.
62. Zhou Y, Cao G, Cai H, Huang H and Zhu X: The effect and clinical significance of FN1 expression on biological functions of gastric cancer cells. Cell Mol Biol (Noisy-le-grand) 66: 191-198, 2020.
63. Cao M, Xiao D and Ding X: The anti-tumor effect of ursolic acid on papillary thyroid carcinoma via suppressing fibronectin-1. Biosci Biotechnol Biochem 84: 2415-2424, 2020.
64. Ding Y, Zhang M, Hu S, Zhang C, Zhou Y, Han M, Li J, Li F, Ni H, Fang S and Chen Q: MiRNA-766-3p inhibits gastric cancer via targeting COL1A1 and regulating PI3K/AKT signaling pathway. J Cancer 15: 990-998, 2024.
65. Markovsky E, Eldar-Boock A, Ben-Shushan D, Baabur-Cohen H, Yeini E, Pisarevsky E, Many A, Aviel-Ronen S, Barshack I and Satchi-Fainaro R: Targeting NCAM-expressing neuroblastoma with polymeric precision nanomedicine. J Control Release 249: 162-172, 2017.
66. Heinly BE and Grant CN: Cell adhesion molecules in neuroblastoma: Complex roles, therapeutic potential. Front Oncol 12: 782186, 2022.